

Activity and stability of RuO₂-coated titanium anodes prepared *via* the alkoxide route

VLADIMIR PANIĆ^{1*#}, ALEKSANDAR DEKANSKI^{1#}, SLOBODAN MILONJIĆ^{2#},
VESNA B. MIŠKOVIĆ-STANKOVIĆ^{3#} and BRANISLAV NIKOLIĆ^{3#}

¹ICTM-IEC, Njegoševa 12, 11000 Belgrade, ²Vinča Institute of Nuclear Sciences, P. O. Box 522, 11001 Belgrade and ³Faculty of Technology and Metallurgy, University of Belgrade, Karnegijeva 4, P. O. Box 3503, YU-11120, Belgrade, Serbia (e-mail: panic@ihm.bg.ac.yu)

(Received 12 May, revised 24 July 2006)

Abstract: Titanium anodes with an active RuO₂ coating of two different thicknesses were prepared from the oxide suspended in ethanol ("ink" method), while the oxide itself was synthesized by the hydrolysis of ruthenium ethoxide in an ethanolic solution (alkoxide route). The morphology of prepared oxide was examined by scanning electron microscopy. The electrochemical properties of the prepared Ti/RuO₂ anodes, involving their cyclic voltammetric behavior in H₂SO₄ and NaCl solutions, activity in the chlorine and oxygen evolution reaction, impedance behavior in H₂SO₄, and stability during electrolysis in dilute chloride solutions, were investigated. The performances of the anodes are compared to those of a Ti/RuO₂ anode prepared by the sol–gel procedure from an oxide sol obtained by the forced hydrolysis of ruthenium chloride in acid solution. The anodes prepared *via* the alkoxide route showed a higher capacitance and activity for the chlorine evolution reaction than the anode prepared by the inorganic sol–gel procedure. The results of the stability test showed that the utilization of the coating active material is better when the anodes were prepared *via* the alkoxide route than *via* the inorganic sol–gel procedure, particularly for anodes with a smaller mass of coating. The different rates of loss of activity indicate a degradation mechanism for the anodes prepared *via* the alkoxide route in which electrochemical dissolution of RuO₂ from the coating surface prevails over the growth of an insulating TiO₂ layer in the coating/Ti substrate interphase. The effect of RuO₂ dissolution from the coating surface increases with increasing coating mass.

Keywords: RuO₂ coating, alkoxide, ink method, ruthenium ethoxide, chlorine evolution, anode stability.

INTRODUCTION

Titanium-supported electroactive oxide coatings based on RuO₂ have been used in the last four decades for the industrial production of chlorine¹ and chlo-

* Corresponding author.

Serbian Chemical Society active member.

doi: 10.2298/JSC0611173P

rate.² Also, the activity of ruthenium oxide has been found to be good for many electrochemical processes,³ with prospective application in the electrooxidation of organics,^{4–6} metal electrowinning⁷ and corrosion protection.^{8,9} In addition, ruthenium oxide exhibits excellent capacitive properties in acid solution due to its pseudocapacitive behavior,^{1,10,11} which makes it a promising candidate for application in electrochemical supercapacitors.^{12–15}

The preparation procedure of the anode is one of the main subjects of investigation, since the conditions during coating formation considerably affect the anode properties. The oxide coating is essentially prepared as a mixed oxide, usually RuO₂, IrO₂ and TiO₂. Noble metal oxides provide the electrocatalytic activity of the coating, while TiO₂ mainly acts as a stabilizing component.^{1,3} Improvement of the coating properties can be achieved using the sol–gel procedure for oxide preparation.^{16–23} The improvement is due to an enlargement of the coating real surface area of the coating, *i.e.* increased contribution of the so-called geometric catalytic factor,²⁴ caused by the formation of finely dispersed oxide particles during the sol–gel procedure. In this manner, the advantage of the sol–gel procedure over the thermal decomposition of metal chlorides,^{1,25} as a standard procedure for coating fabrication, is indicated. The stability of the sol–gel prepared RuO₂–TiO₂ coatings during electrolysis, which can be considerably affected by a changes in the sol–gel preparation conditions,^{22,26} was found to be greater than that of thermally prepared anodes.^{18,22,23} It seems that the anodes prepared by different procedures loose electrocatalytic activity through different pathways.²⁷

Bearing in mind the importance of a controlled formation of the oxide solid phase and the major contribution of RuO₂ to the electrocatalytic activity of the coating, an attempt to prepare a Ti/RuO₂ anode from an organic dispersion was made in this study. The application of an organic oxide dispersion, with a lower surface tension onto a titanium substrate is expected to give a more uniform coating in comparison to the application of an inorganic sol. The basic electrochemical properties of anodes prepared by this, often called, ink method, are reported here and compared to earlier obtained results for a Ti/RuO₂ anode prepared by the sol–gel procedure from an inorganic oxide sol.^{26,28}

EXPERIMENTAL

A dispersion of ruthenium oxide was obtained from ruthenium ethoxide, according to a modified procedure proposed by Komeyama *et al.*¹⁷ and Armelao *et al.*²¹ Ruthenium oxide was prepared from RuCl₃ dissolved in ethanol. Prior to dissolution, commercial RuCl₃·*x*H₂O (Merck) was dried in a nitrogen atmosphere at a temperature of 110 °C for 24 h. The solution was heated to boiling (~76 °C) under nitrogen atmosphere and then a 20 mass % ethanolic solution of sodium ethoxide, NaOEt, (Merck) was slowly dropped into the refluxing solution. The reactants were mixed in the amounts to obtain a 0.1 mol dm⁻³ Ru(OEt)₃ solution. One hour after NaOEt addition, the precipitate (a mixture of RuO_{*x*}H_{*y*} and NaCl) was separated from the solution and washed with distilled water, in order to separate the hydrous ruthenium oxide from NaCl. After drying in air at a temperature of 120 °C for 24 hours, the oxide was suspended in ethanol using an ultrasonic bath (70 kHz). The oxide ink sus-

pension attended satisfactory stability for coating preparation after 45 minutes of ultrasonic treatment.

Titanium rods (3 mm in diameter) were used as supports. The rods were degreased with a saturated ethanolic solution of NaOH and etched in hot HCl solution, rinsed with distilled water and dipped into the oxide suspension up to a height of 1.5 cm. The formed oxide layer on Ti was dried at a temperature of 70 °C. The dipping and drying were repeated until a coating mass of 0.61 or 1.1 mg cm⁻² was reached. The final step of the Ti/RuO₂ anode formation was calcination at a temperature of 450 °C for 1 h, which provide good coating adhesion and crystalline RuO₂ structure.¹⁸

The microscopic appearance of the dried oxide from ethanolic suspension was observed by scanning electron microscopy (SEM) using a JEOL microscope, model JSM-T20 (U_w = 20 kV).

The capacitive behavior of the prepared anodes was investigated by cyclic voltammetry in 1.0 mol dm⁻³ H₂SO₄ and in 0.50 mol dm⁻³ NaCl, pH 2, as well as by electrochemical impedance spectroscopy (EIS) in 1.0 mol dm⁻³ H₂SO₄, while the anode activity in the chlorine and oxygen evolution reaction (CER and OER, respectively) was investigated by potentiostatic polarization measurements in 1.0 mol dm⁻³ H₂SO₄ and in 5 mol dm⁻³ NaCl, pH 2. The capacitive behavior and the CER activity of the anodes prepared *via* the alkoxide route were also registered after the accelerated stability test.

Degradation of the prepared anodes was provoked by an accelerated stability test (AST).^{18,25} The AST was performed by galvanostatic electrolysis in 0.50 mol dm⁻³ NaCl, pH 2, at a current density of 2.0 A cm⁻² with recording the time-dependence of the anode potential. The end of anode service life was seen as a sudden increase in the anode potential. The AST conditions favor oxygen rather than chlorine evolution, which causes the accelerated degradation of the coating.

The electrochemical experiments were performed at room temperature (~25 °C). The surface area of the working electrode was 1.2 cm². A platinum mesh served as the counter electrode and a saturated calomel electrode (SCE) as the reference electrode. All potentials in this paper refer to the SCE scale.

The electrochemical properties of the prepared anodes were compared to a Ti/RuO₂ anode prepared by the sol-gel procedure with the coating mass of 2 mg cm⁻² and the oxide sol obtained by the forced hydrolysis of RuCl₃ in 5 mol dm⁻³ boiling HCl.²⁸ The sol was applied onto Ti plate by multilayer painting, with the same thermal treatment of coating as employed in this work.

RESULTS AND DISCUSSION

Figure 1 shows typical SEM microphotographs of a thin (Fig. 1a) and a thick (Fig. 1b) Ru oxide layer, corresponding to coating masses of 0.61 and 1.1 mg cm⁻², respectively. The appearance of the thin layer surface indicates a less compact structure than that of the thick one. The heterogeneous morphology of the thin layer comprises roughly round islands of diameter between 6 and 7 μm, separated by ≈ 0.5 μm wide cracks. Clusters of uniformly sized, spherical grains of diameter between 0.5 and 1 μm are also seen. The surface of the thick layer has a cracked muddy appearance, with irregularly shaped islands, separated by 0.4 – 0.7 μm-wide cracks. The islands are highly porous, due to a large number of pores with a small orifice diameter. The pores appear to be of uniform size, which indicates the presence of uniformly sized particles in the material.

The cyclic voltammograms of the prepared anodes registered in the H₂SO₄ and in the NaCl solution are shown in Figs. 2. and 3, respectively. Figure 2 also includes the cyclic voltammogram of an anode prepared from an inorganic oxide sol as obtained earlier.²⁸ All the voltammetric curves are of quite similar shape, which

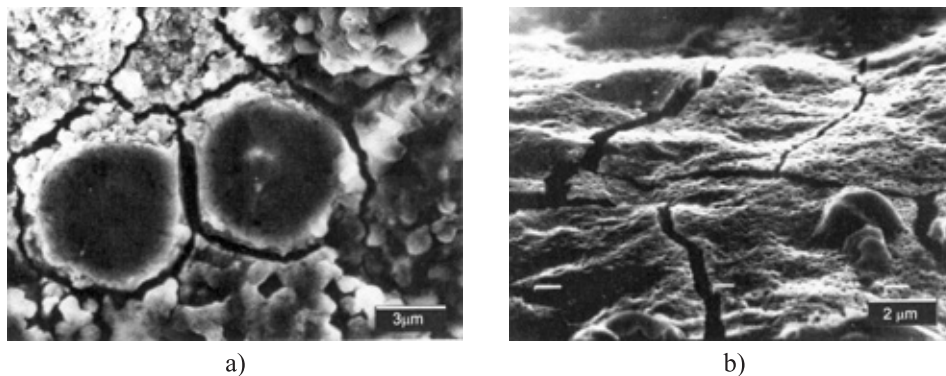


Fig. 1. SEM Microphotographs of (a) thin and (b) thick (angle of incidence: 45°) hydrous ruthenium oxide layer prepared from ruthenium ethoxide.

is usually registered for RuO_2 electrodes.^{1,10} Although the currents do not differ significantly, the highest current are registered for the anode with a thick coating prepared *via* the alkoxide route (Fig. 2), while similar currents were obtained for the thin coating and the coating prepared from an inorganic oxide sol. It can be concluded from Fig. 2 that the anodes have similar electrochemical active surface areas, although considerably smaller coating masses were applied in the ink method than in the inorganic sol-gel procedure. The almost double coating mass of the anodes prepared *via* the alkoxide route did not lead to the appropriate increase in the voltammetric currents, especially in the NaCl electrolyte (Fig. 3).

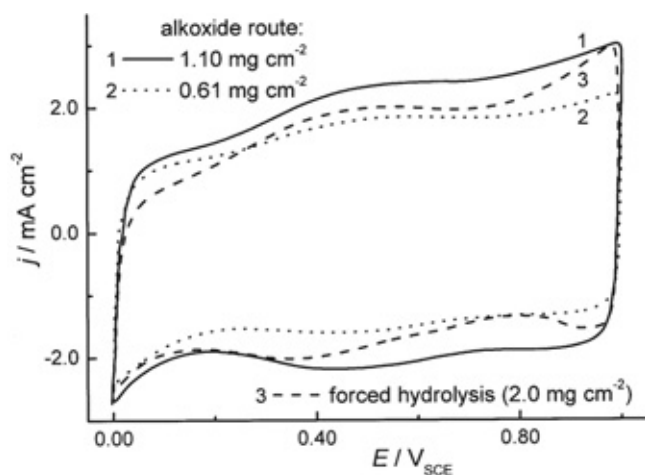


Fig. 2. Cyclic voltammograms of Ti/RuO_2 anodes prepared *via* the alkoxide route and the inorganic sol-gel procedure. Electrolyte: $1.0 \text{ mol dm}^{-3} \text{ H}_2\text{SO}_4$, room temperature. Sweep rate: 50 mV s^{-1} .

The current values registered in the NaCl electrolyte (Fig. 3) are lower than those in the H_2SO_4 electrolyte (Fig. 2), owing to the lower proton concentration in the NaCl electrolyte.¹¹ Protons are involved in several solid-state surface redox transitions of ruthenium species occurring over the whole potential range of electrolyte stability, which are usually schematically written as:^{10,12,29}

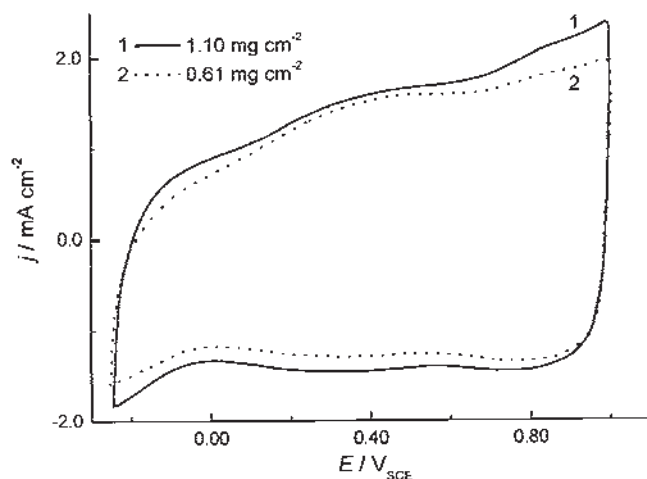


Fig. 3. Cyclic voltammograms of Ti/RuO₂ anodes prepared *via* the alkoxide route. Electrolyte: 0.50 mol dm⁻³ NaCl, pH 2, room temperature, Sweep rate: 50 mV s⁻¹.



This behavior is the origin of the high pseudocapacitance of oxide. The voltammetric charge depends on the applied sweep rate in the voltammetric measurements, due to the porous structure of the coating.¹⁰ The capacitance, obtained from the voltammetric curves (Appendix I), decreases with increasing sweep rate, owing to the different accessibilities of the electrolyte to the outer (directly exposed to the electrolyte) and the inner (within the pores and cracks) surface of the porous coating.^{24,30,31} For the anodes prepared in this work, the capacitance values in the H₂SO₄ electrolyte were higher for the thick coating at all sweep rates, while higher values were obtained for the thin coating in the NaCl electrolyte at low sweep rates (not shown). In general, the capacitance values of the coatings of different mass approach each other as the sweep rate increases.

TABLE I. Overall capacitance, *C*, (in mF cm⁻²) for the thin and thick coating prepared *via* the alkoxide route, obtained from cyclic voltammograms at different sweep rates in the H₂SO₄ and NaCl electrolyte

Electrolyte	Coating mass / mg cm ⁻²	
	0.61	1.10
H ₂ SO ₄	61.8	65.4
NaCl	50.4	37.1

The dependence of the capacitance on the sweep rate can be used to calculate the values of the overall coating capacitance (Appendix I, Eqs. (4) and (5)),^{12,30} which are given in Table I for the thin and thick coatings obtained in the H₂SO₄ and NaCl electrolytes. The values of the overall capacitance in H₂SO₄ for different coating masses were similar. However, in the NaCl electrolyte, a higher value was obtained for the thin coating, although the voltammetric currents in Fig. 3, are higher for the thick coating. This apparent discrepancy originates from the differ-

ence in electrolyte accessibility to the inner part of the coating surface. Da Silva *et al.*,³¹ discussing "the electrochemical porosity" of oxide coatings, showed that the contribution of the inner parts of a coating is more pronounced in supporting electrolytes containing less solvated anions, which participate in the charging of the solution side of the oxide/solution interface. This causes the electrochemical porosity of the thin coating to be higher in the Cl^- than in the SO_4^{2-} electrolyte, as registered in this work, while the inner surface of the thick coating remains inaccessible in both the H_2SO_4 and NaCl electrolyte, even at low sweep rates, owing to its compact structure (Fig. 1b). Higher capacitance values for both the thin and thick coating were registered in the H_2SO_4 than in the NaCl electrolyte. This means that the contribution of the higher proton concentration, which increases the pseudo-capacitance in the H_2SO_4 electrolyte, is more pronounced than the inner surface charging in the NaCl electrolyte.

The Tafel plots for the CER on the anodes prepared *via* the alkoxide route and those obtained earlier²⁸ by the inorganic sol-gel procedure are shown in Fig. 4a. The plots are of the same slope, which is in accordance with the Tafel slope for the CER on RuO_2 -activated titanium anodes reported in the literature.^{1,3,18,32} The currents were larger for the anodes prepared *via* the alkoxide route. If the currents are normalized to the overall coating capacitance (Table I), as a measure of the active surface area,^{24,31} the electrocatalytic activity in the CER is seen. Bearing in mind that the most outer parts of the overall surface of the porous electrodes are active during the gas evolution, the total capacitance registered in the H_2SO_4 electrolyte is used for current normalization. The capacitance registered in the NaCl electrolyte includes the response of the inner surface, which is inactive at the higher overpotentials for the CER and, hence, these capacitance values are less suitable for current normalization.

Figure 4b shows that the anodes of the two different coating masses differ in activity. The thick coating is of slightly higher electrocatalytic activity than the thin one at potentials above 1.07 V, which is rather surprising. The difference is the same as the difference in the measured currents (Fig. 4a), meaning that some other factors affect the coating activity. This idea appears to be closely related only to the CER kinetics on activated titanium anodes, since there is no difference in activity between thick and thin coating in the OER (Fig. 5). One tentative explanation is that, according to the model by Evdokimov for CER on porous anodes,^{33,34} the CER activity on activated titanium anodes can be considerably promoted at higher overpotentials due to the forced micro-convection, since the reaction is controlled by Cl_2 diffusion from the coating surface towards the electrolyte bulk. The increase in activity is assigned to an instant penetration of the electrolyte through the "gas channels" formed at higher overpotentials in the coating pores.³⁴ Since the thick coating is more compact, the promotion in the CER activity by gas channels at higher overpotentials is more pronounced than in the case of the thin coating,

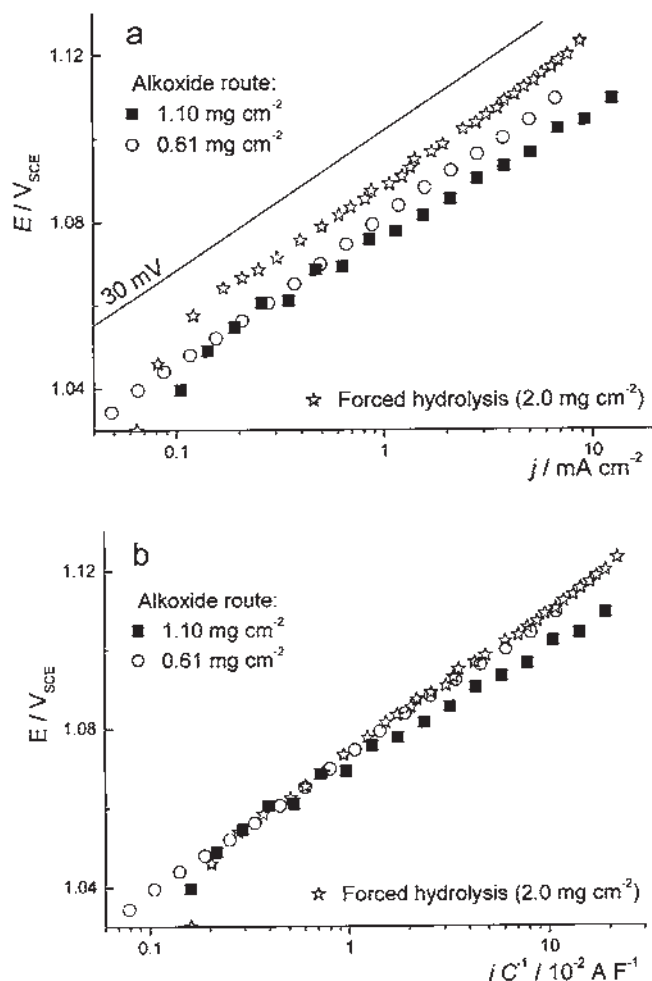


Fig. 4. Tafel plots (a) and normalized Tafel plots (b) for the chlorine evolution reaction on Ti/RuO₂ anodes prepared *via* the alkoxide route and the inorganic sol-gel procedure, in 5 mol dm⁻³ NaCl, pH 2, at room temperature.

with relatively wider pores, where the formation of gas channels and instant penetration of the electrolyte is of lower frequency.

The activity in the OER of the anodes prepared *via* the alkoxide route is illustrated in Fig. 5 by normalized Tafel plots registered in 1.0 mol dm⁻³ H₂SO₄. The Tafel slope of 40 mV dec⁻¹ is within the wide region of slope values between 30 and 70 mV dec⁻¹ usually registered in the OER on oxide-based electrodes.³⁵⁻³⁹ The anodes showed the same activity in the OER, although slightly higher measured currents (not shown) were registered for the thick coating, similar to the CER (Fig. 4a).

The service life performances of the anodes during galvanostatic electrolysis of a dilute chloride solution at 2.0 A cm⁻² in the AST are shown in Fig. 6 as time dependences of the anode potential. The anode with a thick coating prepared *via* the alkoxide route lasts somewhat longer than the thin one, although the onsets of the increase in the potential of the anodes with the thin and thick coating are close. The

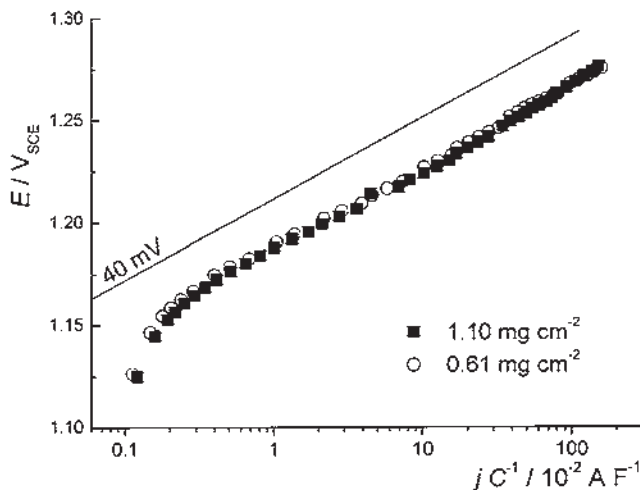


Fig. 5. Tafel plots for the oxygen evolution reaction on Ti/RuO₂ anodes prepared *via* the alkoxide route obtained by polarization measurements in 1.0 mol dm⁻³ H₂SO₄ at room temperature.

longest service life is seen for the anode prepared by the inorganic sol-gel procedure. However, the increase in anode service life is not followed by the proportional increase in the coating mass. At the beginning of electrolysis, the potential decreases with respect to the initial one, E_0 , due to a feature known as "breaking-in",² related to the delayed response of the inner active sites of the coating. This decrease is more pronounced for the anode with the thick coating, owing to its more compact structure. The anode potential is stable until the onset of the coating degradation, caused by an increase in the anode resistance, as will be discussed later on.

The data from Fig. 6 can be discussed from the standpoint of the utilization of the active coating material. It is clear that the utilization of the active material prepared *via* the alkoxide route is considerably better in the case of the thin coating, while the service life of the anode with the thick coating and, particularly, of the anode prepared by the inorganic sol-gel procedure ends before complete exhaustion of the active mate-

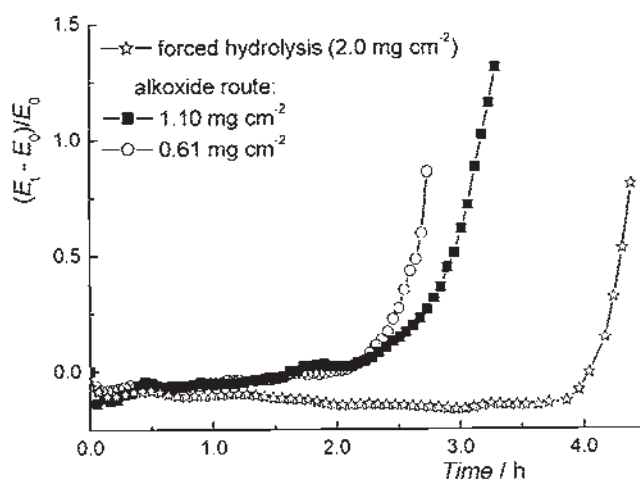


Fig. 6. Time dependence of the relative change in the anode potential, E_t , with respect to the initial, E_0 , at a current density of 2.0 A cm⁻² in 0.50 mol dm⁻³ NaCl, pH 2, for Ti/RuO₂ anodes prepared *via* the alkoxide route and the inorganic sol-gel procedure.

rial. The increase in the anode potential is the consequence of an increased resistance, certainly caused by an increase of the TiO₂ content (which already exists in the coating as a result of calcination during the preparation of the coating). The increase is due to RuO₂ dissolution from the coating surface and/or TiO₂ enrichment in the coating/Ti substrate interphase, owing to substrate oxidation during electrolysis. There is no proportionality between the coating mass and the service life and it can be concluded that the coating porosity affects the rate and mechanism of the degradation process of the coating. The rate of RuO₂ exhaustion for the anode with the thick coating was slower due to its more compact structure, and the electrolyte can hardly access the substrate and its oxidation is consequently slower. The lower rate of the increase in the anode potential implies that this increase is due to an increasing pore resistance of the growing RuO₂-exhausted layer from the coating surface towards the bulk of the coating. On the other hand, the higher rate of increase in the potential of the anode with a thin coating suggests that a progressive enrichment with TiO₂ in the coating/substrate interphase, due to Ti substrate oxidation, occurs.

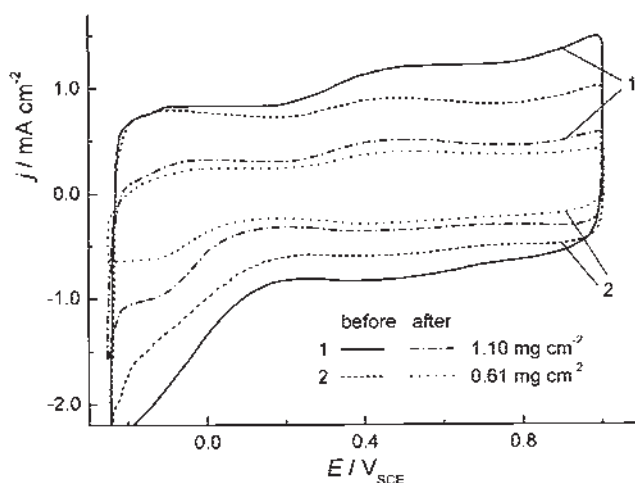


Fig. 7. Cyclic voltammograms of Ti/RuO₂ anodes prepared *via* the alkoxide route in 1.0 mol dm⁻³ H₂SO₄ before and after the accelerated stability test. Sweep rate 20 mV s⁻¹.

The capacitive performance of the anodes after the AST are illustrated in Fig. 7 by cyclic voltammograms in the H₂SO₄ electrolyte. The voltammetric currents decreased as a consequence of the decreased content of active material due to dissolution. The currents of thick coating are still higher than the currents for the thin one. It seemed interesting to compare the capacitance values obtained from the curves in Fig. 7, which are given in Table II. The difference in the capacitance between the thin and thick coating is considerably greater before than after the AST (12.5 and 3.7 mF cm⁻², respectively). The decrease in capacitance during the AST determined at 20 mV s⁻¹, $\Delta_{AST}C_{20}$, is smaller for the thin than for the thick one. However, the relative decrease in the capacitance during the AST is much higher for the thin coating. This supports the consideration concerning the better utilization of the active material in the thin coating and the concluded mechanism of the

degradation of the thin coating, *via* an increasing of the thickness of the insulating TiO₂ layer in the interphase.

TABLE II. The change in the capacitance obtained from cyclic voltammograms in H₂SO₄ at 20 mV s⁻¹, C₂₀, (in mF cm⁻²) for the thin and thick coating, as the consequence of the AST

	Coating mass / mg cm ⁻²	
	0.61	1.10
Before AST	40.3	52.8
After AST	13.5	17.2
$\Delta_{AST}C_{20}$	26.8	35.6

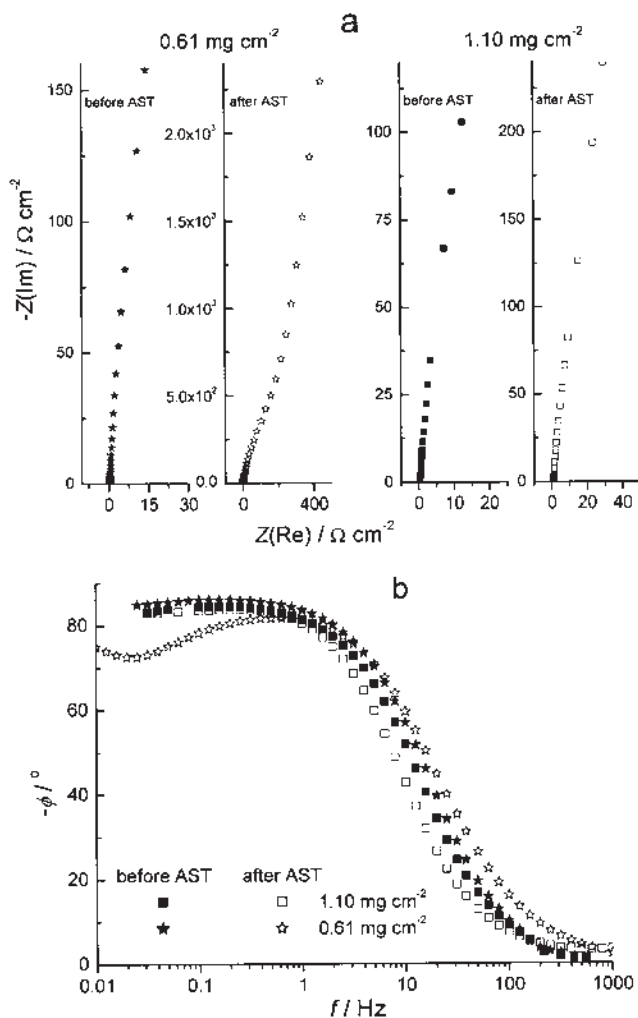


Fig. 8. Complex plane plots (a) and Bode phase angle plots (b) of the EIS data registered in 1.0 mol dm⁻³ H₂SO₄ at a potential of 0.50 V_{SCE}, before and after the accelerated stability test, for Ti/RuO₂ anodes prepared *via* the alkoxide route.

The changes in capacitive behavior and the increase of the resistance of the anodes as a result of the AST can also be seen from EIS measurements. The EIS data of the anodes with thin and thick coatings registered before and after the AST in 1.0 mol dm⁻³ H₂SO₄ at a potential of 0.50 V_{SCE} are shown in Fig. 8. The data are presented as complex plane and Bode phase angle plots. The values of the real and imaginary impedance components were considerably greater after the AST. However, while the values of impedance components were quite similar for both the thick and thin coating before the AST, they were about one order of magnitude higher after the AST for the thin coating. This indicates that a considerable amount of active material still remains in the thick coating after the AST, and that the utilization of the active material of this coating is lower. For the thin coating, the increased anode resistance after the AST is clearly seen as a semicircle-like deviation from capacitive-like behavior.²⁷ This is seen better in the Bode phase angle plot for this anode, since the phase angle dependence shows a broad peak at a frequency of about 1 Hz. The increased resistance is due to the growth of insulating TiO₂ in the bulk of the coating, since the broad peak in the Bode plot appears at a relatively low frequency.²⁷ This kind of deviation from capacitive-like behavior of the EIS data was not registered for the thick coating, in which a significant amount of active material remained, making the capacitive behavior dominant in its EIS response after AST.

CONCLUSION

The morphology of the ruthenium oxide prepared from ruthenium ethoxide (alkoxide route) and the electrochemical properties of Ti/RuO₂ anodes with thin and thick coatings, obtained by the ink method from an ethanolic suspension of the oxide, were investigated. The thick oxide layer had cracked mud structure with nanoporous islands, while the thin layer appeared less compact, with agglomerates of particles having a diameter between 0.5 and 1 μm. Cyclic voltammetry investigations showed that the coatings prepared *via* the alkoxide route had a similar electrochemically active surface area, in spite of the considerable difference in the coating masses. Even with considerably smaller masses of the prepared coating, the coating surface area accessible to the charging/discharging process was similar to that of the coating prepared from an inorganic oxide sol.

The anodes prepared *via* the alkoxide route are more active in the chlorine evolution reaction than the anode prepared from the inorganic oxide sol, due to their larger real surface area. The coating mass on the anode does not influence significantly the anode activity in the chlorine and oxygen evolution reaction at low overpotentials. The more compact thick coating appears to be more active for the chlorine evolution at higher overpotentials, due to forced micro-convection in the pores.

The anode service life is not significantly increased by increasing coating mass. The increase in the coating mass leads to a lower utilization of the active material of the coating during the electrolysis of a chloride solution.

Acknowledgement: This work was financially supported by the Ministry of Science and Environmental Protection of the Republic of Serbia, Contract No. 142061.

ИЗВОД

АКТИВНОСТ И СТАБИЛНОСТ ТИТАНСКИХ АНОДА СА ПРЕВЛАКОМ ОД
ОКСИДА РУТЕНИЈУМА ДОБИЈЕНОМ АЛКОКСИДНИМ ПОСТУПКОМ

ВЛАДИМИР ПАНИЋ,¹ АЛЕКСАНДАР ДЕКАЊСКИ,¹ СЛОБОДАН МИЛОЊИЋ,²
ВЕСНА Б. МИШКОВИЋ-СТАНКОВИЋ³ и БРАНИСЛАВ НИКОЛИЋ³

¹ИХТМ-ЦЕХ, Њеѓошева 12, 11000 Београд, ²Институт за нуклеарне науке "Винча", П. фах 522, 11001 Београд и ³Технолошко-металуришки факултет, Универзитет у Београду, Карнегијева 4, П. фах 5303, 11120 Београд

Титанске аноде са активном превлаком од оксида рутенијума две различите дебљине, формиране су од оксида добијеног хидролизом рутенијум(III)-етоксида у етанолском раствору ("ink" метода). Морфологија добијеног оксида испитивана је скенирајућом електронском микроскопијом. Испитивана су електрохемијска својства формираних анода, која подразумевају циклично-волтаметријско понашање у растворима H₂SO₄ и NaCl, активност у реакцијама издвајања хлора и кисеоника, импедансно понашање и стабилност током електролизе разблажених раствора хлорида. Карактеристике добијених анода упоређене су са карактеристикама аноде формиране сол-гел поступком из оксидног сола добијеног форсираном хидролизом рутенијум(III)-хлорида у киселој средини (5 mol dm⁻³ HCl). Аноде формиране алкоксидним поступком имају већу капацитивност и активност за реакцију издвајања хлора од аноде добијене сол-гел поступком из неорганског сола. Резултати теста стабилности у раствору хлорида показују да је искоришћење активног материјала превлаке такође боље код анода добијених алкоксидним поступком, нарочито за аноду са мањом дебљином превлаке. Резултати указују на то да у механизму губитка активности анода добијених алкоксидним поступком електрохемијско растварање оксида рутенијума са површине превлаке преовлађује у односу на раст изолаторског слоја оксида титана у међуфази превлаке/титанска подлога. Ефект растварања RuO₂ са површине је израженији код превлаке веће дебљине.

(Примљено 12. маја, ревидирано 24. јула 2006)

REFERENCES

1. S. Trassatti, W. O'Grady, in *Advances in Electrochemistry and Electrochemical Engineering*, H. Gerisher, C. W. Tobias, Eds., Wiley, New York, 1981, p. 177
2. A. Cornell, F. Herlitz, 4th *Kurt Schwabe Corrosion Symposium*, Proceedings, Helsinki, Finland, 2004, p. 326
3. S. Trasatti, in *Interfacial Electrochemistry – Theory, Experiment and Applications*, A. Wieckowski, Ed., Marcel Dekker Inc., New York, 1999, p. 769
4. E. O'Sullivan, J. White, *J. Electrochem. Soc.* **136** (1989) 2576
5. C. L. P. S. Zanta, A. R. De Andrade, J. F. C. boodts, *Electrochim. Acta* **44** (1999) 3333
6. V. V. Panić, A. B. Dekanski, T. R. Vidaković, V. B. Mišković-Stanković, B. Ž. Jovanović, B. Ž. Nikolić, *J. Solid State Electrochem.* **9** (2005) 43
7. F. Herlitz, B. Hakansson, 4th *Kurt Schwabe Corrosion Symposium*, Proceedings, Helsinki, Finland, 2004, p. 323
8. K. Darowicki, S. Janicki, *Corr. Sci.* **41** (1999) 1165
9. S. M. A. Shibli, V. S. Gireesh, S. George, *Corr. Sci.* **46** (2004) 819
10. S. Ardizzzone, S. Trasati, *Adv. Colloid Interface Sci.* **64** (1996) 173

11. W. Sugimoto, T. Kizaki, K. Yokoshima, Y. Murakami, Y. Takasu, *Electrochim. Acta* **49** (2004) 313
12. B. E. Conway, *Electrochemical Supercapacitors: Scientific Fundamentals and Technological Applications*, Kluwer Academic/Plenum Publishers, New York, 1999, p. 211
13. T. Jow, J. Zheng, *J. Electrochem. Soc.* **145** (1998) 49
14. M. Ramani, B. Harna, R. White, B. Popov, *J. Electrochem. Soc.* **148** (2001) A374
15. V. Panić, T. Vidaković, S. Gojković, A. Dekanski, B. Nikolić, *Electrochim. Acta* **48** (2003) 3805
16. M. Gugliemi, P. Colombo, V. Rigato, G. Battaglin, A. Boscolo-Boscoletto, A. De Battisti, *J. electrochem. Soc.* **139** (1992) 1655
17. K. Komeyama, S. Shohji, S. Onoue, K. Nishimara, K. Yahikazawa, Y. Takasu, *J. Electrochem. Soc.* **140** (1993) 1034
18. V. Panić, A. Dekanski, S. Milonjić, R. Atanasoski, B. Nikolić, *Colloids Surf. A* **157** (1999) 269
19. A. J. Terezo, E. C. Pereira, *Mater. Lett.* **53** (2002) 339
20. Y. Takasu, Y. Murakami, *Electrochim. Acta* **45** (2000) 4135
21. L. Armelao, D. Barreca, B. Moraru, *J. Non-Cryst. Solids* **316** (2003) 364
22. D. Mitrović, V. Panić, A. Dekanski, S. Milonjić, R. Atanasoski, B. Nikolić, *J. Serb. Chem. Soc.* **66** (2001) 847
23. M. Aparicio, L. C. Klein, *J. Sol-Gel Sci. Technol.* **29** (2004) 81
24. S. Trasatti, *Electrochim. Acta* **36** (1991) 225
25. V. Jovanović, A. Dekanski, P. Despotov, B. Nikolić, R. Atanasoski, *J. Electroanal. Chem.* **339** (1992) 147
26. V. Panić, A. Dekanski, S. Milonjić, R. T. Atanasoski, B. Ž. Nikolić, *Electrochim. Acta* **46** (2000) 415
27. V. V. Panić, A. B. Dekanski, V. B. Mišković-Stanković, S. K. Milonjić, B. Ž. Nikolić, *J. Serb. Chem. Soc.* **68** (2003) 979
28. V. Panić, A. Dekanski, S. K. Milonjić, R. Atanasoski, B. Nikolić, *Mater. Sci. Forum.* **352** (2000) 117
29. M. Vuković, D. Čukman, *J. Electroanal. Chem.* **474** (1999) 167
30. S. Ardizzone, G. Fregonara, S. Trasatti, *Electrochim. Acta* **35** (1990) 263
31. L. M. Da Silva, L. A. De Faria, J. F. C. Boodts, *Electrochim. Acta* **47** (2001) 395
32. L. I. Krishtalik, *Electrochim. Acta* **26** (1981) 329
33. S. V. Evdokimov, *Russ. J. Electrochem.* **36** (2000) 600
34. S. V. Evdokimov, *Russ. J. Electrochem.* **36** (2000) 609
35. Lj. M. Gajić-Krstajić, T. Lj. Trišović, N. V. Krstajić, *Corr. Sci.* **46** (2004) 65
36. G. Lodi, E. Sivieri, A. De Battisti, S. Trasatti, *J. Appl. Electrochem.* **8** (1978) 135
37. P. Castelli, S. Trasatti, F. H. Pollak, W. E. O'Grady, *J. Electroanal. Chem.* **210** (1986) 189
38. A. Terezo, J. Bisquert, E. Pereira, G. Garcia-Belmonte, *J. Electroanal. Chem.* **508** (2001) 59
39. A. de Oliveira-Sousa, P. de Lima-Neto, *J. Braz. Chem. Soc.* **13** (2002) 218.

APPENDIX I. *Calculation of the overall capacitance of porous coatings*

According to the de Levie model for the capacitive response of a porous medium towards a sinusoidal perturbation in time,¹² the part of the total surface of the porous medium which is involved in the capacitive response depends on the morphology and characteristics of the perturbing signal. The penetration depth, z_p , of the signal into the porous media is proportional to the reciprocal square root of the perturbing signal:

$$z_p = \sqrt{\frac{2}{\omega R_p C_{dl}}} \quad (2)$$

where ω is the angular frequency of the perturbing signal, while R_p and C_{dl} are the pore resistance and the double layer capacitance of the coating up to the pore length z_p . According to Equation (2), the penetration depth decreases with angular frequency. In order to obtain capacitive response of the whole porous medium, a perturbing signal of angular frequency:

$$\omega = \frac{64}{R_p C_{dl} l^2} \quad (3)$$

where l is the pore length, should be applied. Adrizzzone *et al.*³⁰ assumed that a similar situation also holds for a potential ramp perturbing signal, so that the registered capacitance should be proportional to the square root of the sweep rate v . Bearing in mind that the whole porous medium is involved in the capacitive response when $v \rightarrow 0$, the overall capacitance of a porous coating C , can be calculated from the intercept of the linear dependence:

$$\frac{1}{C(v)} = \frac{1}{C} + k' \sqrt{v} \quad (4)$$

where $C(v)$ is the capacitance at different sweep rates and k' is a proportionality constant. $C(v)$ is obtained by the integration of the anodic/cathodic branch of a cyclic voltammogram according to the equation:

$$C(v) = \frac{\int_{E'}^E j(E) dE}{Av(E - E')} \quad (5)$$

where E and E' are lower and upper potential limits of the integration of $j(E)$ curve, and A is the geometric surface area of the working electrode.